

Vibronic approach in the theory of the excitonic spectra of molecular crystals

I. J. Lalov and I. Zhelyazkov

Faculty of Physics, Sofia University, BG-1164 Sofia, Bulgaria

(Received 5 February 2007; revised manuscript received 21 May 2007; published 27 June 2007)

The excitonic and vibronic spectra of a molecular chain have been studied on using a complete vibronic approach (without separation in Hilbert subspaces) which has been developed in this paper. The methods of canonical transformations and Green's functions are applied to find out analytical expressions as continued fractions for the linear optical susceptibility near the frequencies of the Frenkel exciton and its first and/or subsequent three vibronic replicas. The approximation of the dynamical theory, i.e., the case of a narrow exciton band compared with the energy of the vibrational quantum, is modified to treat vibronic spectra with totally symmetric phonons by considering both the linear and quadratic exciton-phonon coupling. The excitonic and vibrational parameters for anthracene, naphthalene, and benzene crystals as well as for three other models of molecular chains have been used in calculating the linear absorption spectra of the one-dimensional models of those crystals. The main results concern the shape of the absorption maxima and the manifestations of joint and unbound exciton-phonon configurations in the one-, two-, and three-phonon vibronic spectra depending on the dominant impact of the linear or (and) quadratic exciton-phonon coupling. The picture of the calculated spectra has been compared with the data of previous theoretical studies. It agrees with the available experimental data on the linear absorption in the three aromatic crystals.

DOI: [10.1103/PhysRevB.75.245435](https://doi.org/10.1103/PhysRevB.75.245435)

PACS number(s): 71.35.Aa, 73.20.Mf, 77.84.Jd, 78.40.Me

I. INTRODUCTION

The spectra of the electronic excitations of molecular systems studied over several decades manifest both pure excitations (excitons) as well as their vibronic replicas.¹⁻³ The molecular linear absorption spectra contain the well-known vibronic progression which corresponds to electronic excitations of the molecule, electronic excitation plus one-, two-, three-, etc., quanta of intramolecular vibrations.⁴⁻⁷ The excitonic and vibronic spectra of the molecular crystals are more complicated because of Davydov's splitting¹ and the various configurations of the exciton and vibrational quanta, notably joint configurations in which the electronic excitation and the intramolecular phonons propagate through the crystal as a whole¹ and configurations of many-particle (MP) states associated with separate unbound propagation of quasiparticles.^{2,3,8,10} The structure of vibronic spectra and their manifestation in the linear and nonlinear optical phenomena^{3,8,9,11,12} of molecular crystals are governed by the exciton-phonon coupling. However, the treatment of a multiparticle problem such as the vibronic spectra of molecular crystals and helical polymers^{9,13} needs some approximations such as the approximation of joint configurations,¹ the approximation of the dynamical theory of vibronics, and the separation of the vibronic region on Hilbert subspaces of pure excitons, one-phonon, two-phonon, three-phonon, and so on vibronics,^{3,8} as well as calculations of the vibronic coupling⁹ and those of the phonon clouds' distribution¹⁴ and other approaches.

In this paper, we avoid the vibronics' separation into complexes of fixed number of vibrational quanta. Such a separation neglects the mutual influence of different complexes. Our approach might be called a vibronic approach and it connects the excitonic and vibronic spectra, but preserves and modifies the assumptions of the dynamical theory of vibronic spectra.^{3,8} Our complex treatment of the vibronic

spectra follows also the ideas of the well-known paper by Philpott;⁹ however, we use a different formalism and consider multiphonon vibronics.

In our paper, we consider a linear problem for connected excitonic (Frenkel exciton) and vibronic spectra in a one-dimensional molecular stack. The most essential approximation is the assumption for relatively weak intermolecular transfer of the Frenkel exciton (the corresponding transfer integral is supposed to be several times smaller compared with the energy of the vibrational quantum). This assumption only is sufficient for calculating the vibronic spectra near the frequencies of a pure Frenkel exciton and its vibronic replicas on using the methods of the canonical transformations and Green's functions (at $T=0$). As usual, we study the linear exciton-phonon coupling as the main coupling mechanism but the quadratic exciton-phonon coupling is taken into account, too, through the changes of the vibrational frequency in the excited molecule.^{2,3,8,10}

The organization of the paper is as follows: Sec. II is devoted to the canonical transformation of the vibronic Hamiltonian and the operator of the transition dipole moment. Sections III and IV contain the core of our vibronic approach, notably the calculation of the Green's functions which enter the expressions for the linear optical susceptibility and the linear absorption spectra near the frequencies of Frenkel exciton and its first three vibronic replicas (Sec. IV). In Sec. V, we use those expressions and the excitonic and phonon's parameters of the most studied aromatic crystals—anthracene, naphthalene, and benzene^{2,3}—to model their linear absorption spectra. In Sec. VI we apply the same expressions in calculating the vibronic spectra of three hypothetical one-dimensional models studied in Ref. 9. Section VII summarizes the results obtained. In the Appendix, we introduce the main formulas of Ref. 10 used in an alternative calculation of the absorption spectra.

II. VIBRONIC HAMILTONIAN

We consider the excitations in a linear chain of regularly arranged molecules $n=1,2,\dots,N$. It corresponds to those stacks in which the molecules are situated at a distance b , closer than their neighbors in the perpendicular plane.¹⁵ We treat the case of one excited electronic state of the molecule which forms in the stack a Frenkel exciton (FE) of excitation energy E_F and transfer integral L between the neighbor molecules, as well as the case with one intramolecular vibration of frequency ω_0 in a nonexcited molecule. Our initial Hamiltonian can be represented as follows:

$$\hat{H} = \sum_n E_F B_n^+ B_n + \sum_{n,n'} L(\delta_{n',n+1} + \delta_{n',n-1}) B_n^+ B_{n'} + \sum_n \hbar \omega_0 a_n^+ a_n + \hat{H}_{\text{ex-phon}}. \quad (1)$$

Here, B_n (B_n^+) is the annihilation (creation) operator of Frenkel exciton on molecule n , and a_n (a_n^+) is the annihilation (creation) operator of one vibrational quantum on the same molecule n .

The operator $\hat{H}_{\text{ex-phon}}$ of exciton-phonon coupling can be represented by using the dimensionless phonon normal coordinate

$$X_n = a_n + a_n^+. \quad (2)$$

The linear and quadratic exciton-phonon coupling is expressed in the following way:¹⁵

$$\hat{H}_{\text{ex-phon}} = \sum_n \hbar \omega_0 B_n^+ B_n (dX_n + eX_n^2). \quad (3)$$

The dimensionless parameter d describes the displacement of the nuclei's equilibrium positions in a molecule with FE, while the parameter e describes the changes of the parabolic potential of vibrating nuclei in the excited molecule.

The operator (3) can be eliminated by using the canonical transformation^{8,10}

$$\hat{H}_1 = \exp(Q) \hat{H} \exp(-Q), \quad (4)$$

where

$$Q = \sum_n \tau B_n^+ B_n [a_n^2 - (a_n^+)^2 + \theta(a_n - a_n^+)], \quad (5)$$

in which

$$\exp(-4\tau) = \sqrt{1+4e}, \quad \theta = -\frac{2d}{(1+4e)[\exp(2\tau) - 1]}. \quad (6)$$

We introduce the vibronic operators

$$V_n = \exp(Q) B_n \exp(-Q) \quad (7)$$

and find the following vibronic Hamiltonian:

$$\hat{H}_1 = \sum_n \left[E_F - \frac{d^2}{1+4e} \hbar \omega_0 + \frac{1}{2} \hbar \Delta \omega \right] V_n^+ V_n + \sum_n \hbar \omega_0 a_n^+ a_n + \sum_{n,n'} L(\delta_{n',n+1} + \delta_{n',n-1}) V_n^+ V_{n'} + \sum_n \hbar \Delta \omega V_n^+ V_n a_n^+ a_n, \quad (8)$$

where

$$\Delta \omega = \omega_0 (\sqrt{1+4e} - 1). \quad (9)$$

In this way, the magnitudes of the parameter e of the quadratic coupling are correlated with the relative frequency shift $\Delta \omega / \omega_0$ of the vibration in the excited molecule. In aromatic solids, that relative shift (more frequently $\Delta \omega / \omega_0 < 0$) exceeds 10% very rarely^{2,3} and thus

$$\Delta \omega / \omega_0 \approx 2e, \quad |e| \ll 1. \quad (10)$$

The Hamiltonian \hat{H}_1 is basic for our studies. Using Eq. (6) and inequality (10), we reduce the quantity Q to an expression which contains only linear terms in the operators a_n, a_n^+ , i.e.,

$$Q \approx \sum_n B_n^+ B_n \xi (a_n^+ - a_n) \quad (11)$$

since $\tau \approx -e/2$ and for aromatic solids $\tau \lesssim 0.02$. The quantity

$$\xi = -\tau \theta \approx d/(1+4e) \quad (12)$$

can be interpreted as a renormalized constant of the linear exciton-phonon coupling. Accordingly, in expression (8) we substitute $d^2/(1+4e) \approx \xi^2$.

For calculating the linear optical susceptibility, we need the operator of transition dipole moment which in the case of a dipole active FE can be expressed as

$$\hat{P}_1 = \sum_n \mathbf{P}_F (B_n^+ + B_n) \quad (13)$$

and it is transformed to the operator

$$\hat{P} = \sum_n \mathbf{P}_F (V_n^+ + V_n). \quad (14)$$

Then, the linear optical susceptibility χ_{ij} can be presented^{1,16} through the operator (14)

$$\chi_{ij} = \lim_{\varepsilon \rightarrow 0} \left\{ -\frac{1}{2\hbar V} [\Phi_{ij}(\omega + i\varepsilon) + \Phi_{ij}(-\omega + i\varepsilon)] \right\}, \quad (15)$$

with

$$\Phi_{ij} = -i\theta(t) \langle 0 | P_i(t) P_j(0) + P_j(t) P_i(0) | 0 \rangle, \quad (16)$$

where V is the crystal's volume. The Green's function (16) has been calculated as average over the ground state $|0\rangle$ taking into account the large values of the FE's energy and that of the vibrational quantum, $E_F, \hbar \omega_0 \gg kT$.

III. CALCULATION OF THE VIBRONIC GREEN'S FUNCTIONS

For calculating the linear optical susceptibility (15), we need the Fourier component in the frequency and momentum space of the following Green's function:

$$G_n(t) = -i\theta(t)\langle 0|V_n(t)\sum_{n_1}V_{n_1}^+(0)|0\rangle, \quad (17)$$

which can be calculated using the standard procedure of differentiation of Eq. (17) with respect to time and bearing in mind the Hamiltonian (8). It is not difficult to find out the following commutation rules for operators V_n , V_n^+ , a_n , a_n^+ (see Ref. 17):

$$V_nV_{n_1}^+ - V_{n_1}^+V_n = \delta_{nn_1}, \quad (18a)$$

$$V_na_{n_1} - a_{n_1}V_n = \xi\delta_{nn_1}V_n, \quad (18b)$$

$$V_na_{n_1}^+ - a_{n_1}^+V_n = \xi\delta_{nn_1}V_n \quad (18c)$$

(recall that a_n and a_n^+ are boson operators).

We obtain the following chain for the Fourier components of Green's functions:

$$(\hbar\omega - E'_F)G_n = 1 + L(G_{n+1} + G_{n-1}) + \hbar\omega_1\xi G_{n,n}^{(1)}, \quad (19)$$

$$\begin{aligned} (\hbar\omega - E'_F - \hbar\omega_0)G_{n,n_1}^{(1)} &= L(G_{n+1,n_1}^{(1)} + G_{n-1,n_1}^{(1)}) + \hbar\Delta\omega G_{n,n}^{(1)}\delta_{nn_1} \\ &+ \hbar\omega_1\xi(G_n + G_{n,n_1}^{(2)}), \end{aligned} \quad (20)$$

$$\begin{aligned} (\hbar\omega - E'_F - 2\hbar\omega_0)G_{n,n_1n_2}^{(2)} &= L(G_{n+1,n_1n_2}^{(2)} + G_{n-1,n_1n_2}^{(2)}) \\ &+ \hbar\Delta\omega(G_{n,n_1n_2}^{(2)}\delta_{nn_1} + G_{n,n_1n}^{(2)}\delta_{nn_2}) \\ &+ \hbar\omega_1\xi(G_{n,n_1}^{(1)} + G_{n,n_2}^{(1)} + G_{n,n_1n_2n}^{(3)}). \end{aligned} \quad (21)$$

(and similar equations for $G^{(3)}, G^{(4)}, \dots$). In these expressions, $G_{n,n_1n_2\cdots n_m}^{(m)}$ is the Fourier component of the following Green's function:

$$G_{n,n_1n_2\cdots n_m}^{(m)} = -i\theta(t)\langle 0|a_{n_1}a_{n_2}\cdots a_{n_m}V_n(t)\sum_{n_1}V_{n_1}^+(0)|0\rangle. \quad (22)$$

E'_F and ω_1 are equal to

$$E'_F = E_F + \hbar\Delta\omega(\xi^2 + 1/2), \quad \omega_1 = \omega_0 + \Delta\omega. \quad (23)$$

As usual, we introduce the spatial Fourier components of Green's functions:

$$\begin{aligned} G_{n,n_1n_2\cdots n_m}^{(m)} &= \frac{1}{N^{m+1}} \sum_{k_1\cdots k_m, k} G^{(m)}(k_1, k_2, \dots, k_m; k) \exp[i(k_1n_1 \\ &+ \cdots + k_mn_m + kn)]. \end{aligned} \quad (24)$$

In the processes of linear absorption, because of the smallness of the wave vector of the absorbed photon, the following relation holds:

$$k_1 + k_2 + \cdots + k_m + k = 0. \quad (25)$$

We find the following equations for the Fourier components of Green's functions (19)–(21):

$$(\hbar\omega - E'_F - 2L)G(k=0) = 1 + \xi\hbar\omega_1 \sum_k G^{(1)}(k, -k), \quad (26)$$

$$\begin{aligned} (\hbar\omega - E'_F - 2L \cos kb - \hbar\omega_0)G^{(1)}(k, -k) &= \xi\hbar\omega_1 G(k=0) \\ &+ \hbar\Delta\omega \sum_k G^{(1)}(k, -k) + \xi\hbar\omega_1 \sum_{k_2} G^{(2)}(k, k_2; -k - k_2), \end{aligned} \quad (27)$$

$$\begin{aligned} (\hbar\omega - E'_F - 2L \cos kb - 2\hbar\omega_0)G^{(2)}(k_1, k_2; k) &= \xi\hbar\omega_1 \sum_{k_3} G^{(3)} \\ &\times (k_1, k_2, k_3; k) + \xi\hbar\omega_1 [G^{(1)}(k_1; -k_1) + G^{(1)}(k_2; -k_2)] \\ &+ \hbar\Delta\omega \left[\sum_{k'_2} G^{(2)}(k_1, k'_2; -k_1 - k'_2) \right. \\ &\left. + \sum_{k'_1} G^{(2)}(k'_1, k_2; -k'_1 - k_2) \right], \end{aligned} \quad (28)$$

$$\begin{aligned} (\hbar\omega - E'_F - 2L \cos kb - 3\hbar\omega_0)G^{(3)}(k_1, k_2, k_3; k) &= \xi\hbar\omega_1 \left[\sum_{k'_4} G^{(4)}(k_1, k_2, k_3, k'_4; k) + G^{(2)}(k_1, k_2; -k_1 - k_2) \right. \\ &\left. + G^{(2)}(k_1, k_3; -k_1 - k_3) + G^{(2)}(k_2, k_3; -k_2 - k_3) \right] \\ &+ \hbar\Delta\omega \left[\sum_{k'_3} G^{(3)}(k_1, k_2, k'_3; -k_1 - k_2 - k'_3) \right. \\ &\left. + \sum_{k'_1} G^{(3)}(k'_1, k_2, k_3; -k'_1 - k_2 - k_3) + \sum_{k'_2} G^{(3)}(k_1, k'_2, k_3; \right. \\ &\left. - k_1 - k'_2 - k_3) \right]. \end{aligned} \quad (29)$$

Now, we turn to the dynamic approach and suppose that the inequality

$$|2L \cos kb| \ll \hbar\omega_0 \quad (30)$$

holds. As a first step, we will look at the solutions to Eqs. (26)–(29) in the frequency region of one-phonon vibronic, as a second step, of two-phonon vibronic, and so forth. Hence, only one coefficient would be resonant, e.g., $|\hbar\omega - E'_F - 2L \cos kb - \hbar\omega_0| \ll \hbar\omega_0$ for the one-phonon vibronic, whereas the other coefficients like $\hbar\omega - E'_F - 2L \cos kb - 2\hbar\omega_0$ or $\hbar\omega - E'_F - 2L \cos kb - 3\hbar\omega_0$ and so on possess absolute values $\approx \hbar\omega_0, 2\hbar\omega_0, \dots$ and thus they vary weakly with k [see inequality (30)]. We preserve the dispersion term $2L \cos kb$ in that equation which describes a particular frequency region, i.e., in Eq. (27) for one-phonon vibronic, in Eq. (28) for two-phonon vibronic, etc., and neglect the same terms in all other equations [Eqs. (26)–(29)]. In such a way, we take into account the influence of the excitonic transfer on the vibronic with one phonon, then with two phonons, and so on.

Modified according to this approach, Eqs. (26)–(29) represent an infinite chain of degenerate integral equations

which can be truncated for some number m if ratios

$$\xi\hbar\omega_1/(\hbar\omega - E'_F - m\hbar\omega_0) \quad \text{and} \quad \hbar\Delta\omega/(\hbar\omega - E'_F - m\hbar\omega_0)$$

could be considered as negligible ones. Supposing that $G^{(m)} \approx 0$, we find solutions for $G^{(m-1)}$, $G^{(m-2)}$ up to $G(k=0)$ which enters the expression for the linear optical susceptibility. The expression for $G(k=0)$ represents a terminated continued fraction. In the most simple case of a nontransferable electronic excitation ($L \equiv 0$) function $G(k=0)$ has the following form:

$$G(k=0) = \frac{1}{\hbar\omega - E'_F - \frac{\xi^2\hbar\omega_1^2}{\omega - E'_F/\hbar - \omega_1 - \frac{2\xi^2\omega_1^2}{\omega - E'_F/\hbar - 2\omega_1 - \dots}}}. \quad (31)$$

We recall again the main features of our vibronic approach.

(1) We use the modified dynamic approach [see inequality (30)], but without an entire separation of vibronics with zero, one, two, and so on phonons.

(2) The linear exciton-phonon coupling must be dominant, whereas the quadratic coupling influences the vibra-

tional frequency in the excited molecule only. There are no limitations on the values of the linear coupling constant; however, in the case of a strong linear coupling we need the longer chain of equations (26)–(29).

(3) The different solutions are valid for the vibronics with a fixed number of intramolecular vibrational quanta. This approach can effectively be applied in calculating vibronics with one, two, three, and four phonons simultaneously with pure excitonic spectra. Hence, the vibronic approach makes the applications of the dynamic theory wider (compare with Refs. 3, 8, and 10).

IV. GREEN'S FUNCTIONS FOR VIBRONICS WITH ONE, TWO, AND THREE VIBRATIONAL QUANTA

This section contains expressions for the Green's functions $G(k=0)$ derived by the methods of the previous section and applicable in the following three frequency regions.

(i) One-phonon vibronic spectrum:

$$G_{1p}(k=0) = \frac{1}{\hbar\omega - E'_F - 2L - \frac{\xi^2\hbar\omega_1^2 S_1}{1 - MS_1}}, \quad (32)$$

where

$$S_1 = \frac{1}{N} \sum_k \frac{1}{\hbar\omega - E'_F - \hbar\omega_0 - 2L \cos kb - \frac{\hbar\xi^2\omega_1^2}{\omega - E'_F/\hbar - 2\omega_0 - \Delta\omega - \frac{2\xi^2\omega_1^2}{\omega_{33}}}}, \quad (33)$$

$$\omega_{33} = \omega - E'_F/\hbar - 3\omega_0 - 2\Delta\omega - \frac{3\xi^2\omega_1^2}{\omega - E'_F/\hbar - 4\omega_0 - 3\Delta\omega - \dots}, \quad (34)$$

$$M = \hbar\Delta\omega + \xi^2\hbar\omega_1^2 \left[\frac{2}{\omega - E'_F/\hbar - 2\omega_1 - \frac{3\xi^2\omega_1^2}{\omega_{34}}} - \frac{1}{\omega - E'_F/\hbar - 2\omega_0 - \Delta\omega - \frac{2\xi^2\omega_1^2}{\omega_{33}}} \right], \quad (35)$$

$$\omega_{34} = \omega - E'_F/\hbar - 3\omega_1 - \frac{4\xi^2\omega_1^2}{\omega - E'_F/\hbar - 4\omega_1 - \dots}. \quad (36)$$

(ii) Two-phonon vibronic spectrum:

$$G_{2p}(k=0) = \frac{1}{\hbar\omega - E'_F - 2L - \frac{\xi^2\hbar\omega_1^2}{\omega - E'_F/\hbar - \omega_1 - \frac{2\xi^2\omega_1^2 S_2}{1 - FS_2}}}, \quad (37)$$

where

$$S_2 = \frac{1}{N} \sum_k \frac{1}{\hbar\omega - E'_F - 2\hbar\omega_0 - 2L \cos kb - \frac{\xi^2 \hbar \omega_1^2}{\omega - E'_F/\hbar - 3\omega_0 - \Delta\omega - \frac{2\xi^2 \omega_1^2}{\omega_{41}}}}, \quad (38)$$

$$\omega_{41} = \omega - E'_F/\hbar - 4\omega_0 - 2\Delta\omega - \frac{3\xi^2 \omega_1^2}{\omega - E'_F/\hbar - 5\omega_0 - 3\Delta\omega - \frac{4\xi^2 \omega_1^2}{\dots}}, \quad (39)$$

$$F = 2\hbar\Delta\omega + \xi^2 \hbar \omega_1^2 \left[\frac{3}{\omega - E'_F/\hbar - 3\omega_1 - \frac{4\xi^2 \omega_1^2}{\omega - E'_F/\hbar - 4\omega_1 - \frac{5\xi^1 \omega_1^2}{\dots}}} - \frac{1}{\omega - E'_F/\hbar - 3\omega_0 - \Delta\omega - \frac{2\xi^2 \omega_1^2}{\omega - E'_F/\hbar - 4\omega_0 - 2\Delta\omega - \frac{3\xi^2 \omega_1^2}{\dots}}} \right]. \quad (40)$$

(iii) Three-phonon vibronic spectrum:

$$G_{3p}(k=0) = \frac{1}{\hbar\omega - E'_F - 2L - \frac{\xi^2 \hbar \omega_1^2}{\omega - E'_F/\hbar - \omega_1 - \frac{2\xi^2 \omega_1^2}{\omega - E'_F/\hbar - 2\omega_1 - D_3}}}, \quad (41)$$

where

$$D_3 = \frac{3\xi^2 \omega_1^2 S_3}{1 - ES_3}, \quad (42)$$

$$S_3 = \frac{1}{N} \sum_k \frac{1}{\hbar\omega - E'_F - 3\hbar\omega_0 - 2L \cos kb - \frac{\xi^2 \hbar \omega_1^2}{\omega - E'_F/\hbar - 4\omega_0 - \Delta\omega - \frac{2\xi^2 \omega_1^2}{\omega_{51}}}}, \quad (43)$$

$$\omega_{51} = \omega - E'_F/\hbar - 5\omega_0 - 2\Delta\omega - \frac{3\xi^2 \omega_1^2}{\omega - E'_F/\hbar - 6\omega_0 - 3\Delta\omega - \frac{4\xi^2 \omega_1^2}{\dots}}, \quad (44)$$

$$E = 3\hbar\Delta\omega + \xi^2 \hbar \omega_1^2 \left[\frac{4}{\omega - E'_F/\hbar - 4\omega_1 - \frac{5\xi^2 \omega_1^2}{\omega - E'_F/\hbar - 5\omega_1 - \frac{6\xi^2 \omega_1^2}{\dots}}} - \frac{1}{\omega - E'_F/\hbar - 4\omega_0 - \Delta\omega - \frac{2\xi^2 \omega_1^2}{\omega - E'_F/\hbar - 5\omega_0 - 2\Delta\omega - \frac{3\xi^2 \omega_1^2}{\dots}}} \right]. \quad (45)$$

The denominators (\dots) in Eqs. (32)–(45) represent continuation of the expressions for the corresponding quantities changing the numerical coefficients by one at each next step of the ladder. The lowest step [after the truncation of Eqs.

(26)–(29)] does not contain the term with $\xi^2 \omega_1^2$.

In all the cases, the linear optical susceptibility is expressed (with axis x being directed along the transition dipole moment \mathbf{P}_F) as follows:

TABLE I. Model parameters of Frenkel excitons and of totally symmetrical vibrations of some aromatic crystals.

Crystal	Excitonic level of a molecule (experiment) $E_F^{(0)}$ (cm^{-1})	Excitonic transfer integral L (cm^{-1})	Vibr. freq. in nonexcited molecule ω_0 (cm^{-1})	Constant of linear coupling ξ^2	Shift of the vibr. freq. in exc. molecule $\Delta\omega$ (cm^{-1})
Anthracene	25 000	117	1400	0.9	0
Benzene	37 800	15	992	1.4	-69
Naphthalene	31 500	45	760	0.4	-58

$$\chi_{xx} = -\frac{P_F^2 N}{\hbar V} G(k=0). \quad (46)$$

The linear absorption spectra will be calculated in the next section as imaginary parts of the Green's functions (31), (32), (37), and (41) providing frequency ω with a small imaginary part which determines the final width of the excitonic and vibrational levels.

V. MODEL OF ABSORPTION SPECTRA OF SOME AROMATIC CRYSTALS

In modeling the absorption spectra of aromatic crystals, we introduce their excitonic and vibrational parameters (see Table I) evaluated as a result of analysis of both experimental data and theoretical arguments.^{2,3,5-7,18} We stress on the limited applicability of our one-dimensional model to the three-dimensional anisotropic aromatic crystals. Nevertheless, our calculations make clearer the general structure of the excitonic and vibronic spectra, as well as the magnitude of the absorption coefficient, especially near the frequencies of vibronics with one, two, and three phonons of the totally symmetric vibrations of aromatic compounds.

The calculations at $L=0$ [see formula (31)] can be considered as a checking point because their results must coincide with the vibronic progression in the spectra of isolated molecules. We have calculated the values of the vibronic Green's function (31) for the parameters of three aromatic compounds using ten steps in the denominator of Eq. (31). The amplitudes of the maxima $n=0, 1, 2, \dots$ really follow the progression rule (n is the number of vibrational quanta)

$$A_n \sim \exp(-\xi^2) \xi^{2n}/n!, \quad (47)$$

but the equal distance between the successive vibronic levels ($n, n-1$), which must be equal to $\omega_1 = \omega_0 + \Delta\omega$, can be obtained by introducing in Eq. (31) a longer ladder, especially in the cases with $\xi^2 > 1$.

Our results at $L \neq 0$ for the frequencies of the Frenkel exciton and of its three vibronic replicas [Eqs. (32), (37), and (41)] have been compared with the results of Ref. 10 which concern excitonic and one-phonon vibronic spectra in one-dimensional molecular chain. Davydov and Serikov¹⁰ make, in fact, a transformation of the Hamiltonian (8), expanding the operator exponents (7), of the vibronic operators and reducing that Hamiltonian to one which preserves the total

numbers of excitons and of phonons in the crystal (see also Refs. 3 and 8):

$$\begin{aligned} \hat{H}_2 = & \sum_n \left[E_F - \xi^2 \hbar \omega_0 + \frac{1}{2} \hbar \Delta\omega \right] B_n^+ B_n + \sum_n \hbar \omega_0 a_n^+ a_n \\ & + \sum_{nn'} L (\delta_{n', n+1} + \delta_{n', n-1}) B_n^+ B_{n'} [1 + \xi^2 (a_n^+ a_{n'} + a_n^+ a_{n'} \\ & - a_n^+ a_n - a_{n'}^+ a_{n'})] + \sum_n \hbar \Delta\omega B_n^+ B_n a_n^+ a_n. \end{aligned} \quad (48)$$

The corresponding formulas for the linear optical susceptibility are given in the Appendix.

In our calculations, the normalized excitonic level E'_F is a free parameter and we fit its value according to the following rule: the excitonic level, calculated from formula (32), occupies position $E_F^{(0)} + 2L$ which corresponds to the experimentally observed excitonic level. We introduce that value of E'_F in the other two formulas [Eqs. (37) and (41)] and obtain practically the same position and amplitude of the excitonic absorption line (see Fig. 1).

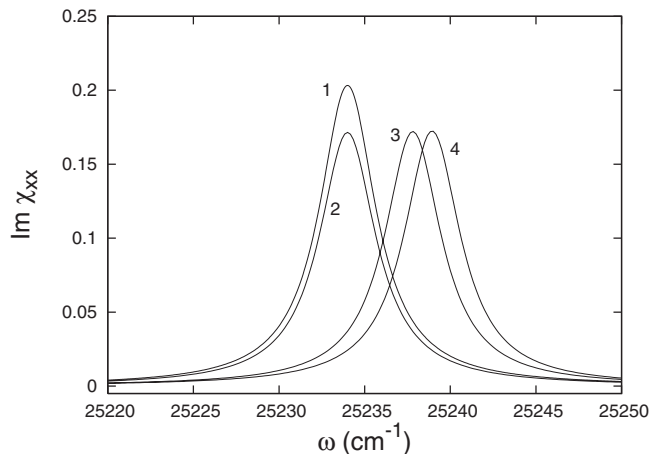


FIG. 1. Linear absorption spectra for one-dimensional model of anthracene's crystal calculated as the imaginary part of Eq. (46) [in arbitrary units; $P_F^2 N / (\hbar V)$ is taken to be equal to 1]. The spectrum of FE, $E'_F + 2L$ ($E_F^{(0)} = 25\,000 \text{ cm}^{-1}$, $L = 117 \text{ cm}^{-1}$), is calculated by using the following formulas: Eq. (A1) for curve 1, Eq. (32) for curve 2, Eq. (37) for curve 3, and Eq. (41) for curve 4. The quantity E'_F in formula (32) is fitted and thus the frequencies of absorption maxima of curves 1 and 2 coincide.

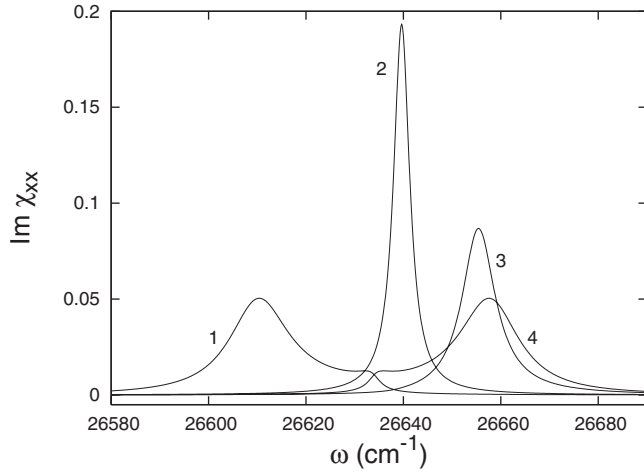


FIG. 2. One-phonon vibronic region of the linear absorption spectra for anthracene. Curve 1 is calculated according to Davydov-Serikov (DS) model with $L=117 \text{ cm}^{-1}$ [formula (A1), Ref. 10], curve 2 is produced by using the approach of the present paper [formula (32), $L=117 \text{ cm}^{-1}$], curve 3 is according to Eq. (32) with $L=-117 \text{ cm}^{-1}$, and curve 4 is generated by the DS model for the same negative value of L .

We calculate the absorption spectra for three crystals introducing data from Table I, the imaginary part $i\delta$ ($\delta=2 \text{ cm}^{-1}$) of the frequency ω , and positive and negative signs of the quantity L .

A. Model of anthracene absorption spectra

According to Table I, the linear exciton-phonon coupling is manifesting only in the vibronic spectra of anthracene because $\Delta\omega=0$. The estimation of exciton transfer integral L has been done using the data for the longitudinal-transversal splitting^{2,3} and shows relatively big transferability of the FE in anthracene. Thus, the excitonic band is wide that can cause the appearance of wide vibronic lines corresponding to

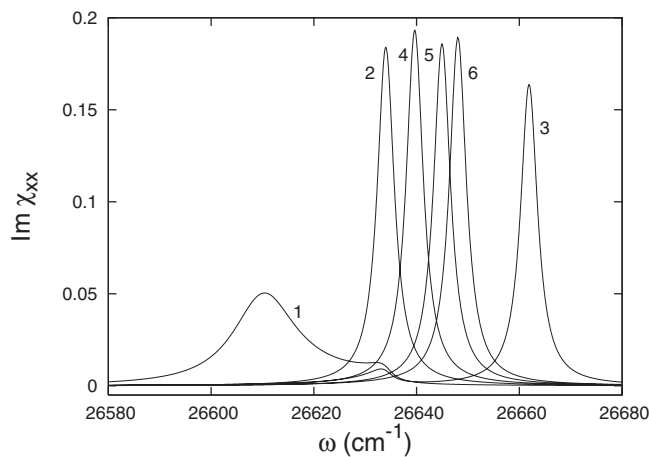


FIG. 3. One-phonon vibronic region of anthracene. Curves 1, 2, and 3 are calculated according to the DS model with $L=117 \text{ cm}^{-1}$ for $\xi^2=0.9, 1,$ and $1.1,$ respectively. The vibronic approach of the present paper for the same values of L and ξ^2 yields curves 4, 5, and 6.

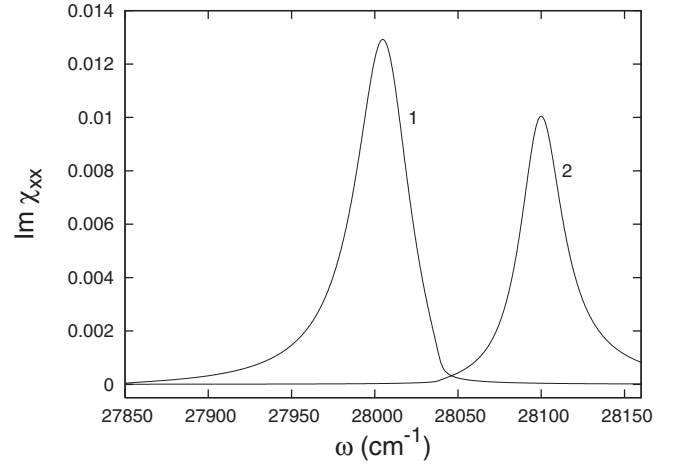


FIG. 4. Two-phonon vibronic region of anthracene at $\xi^2=0.9$ for two values of the excitonic transfer integral L equal to 117 cm^{-1} for curve 1 and -117 cm^{-1} for curve 2, respectively.

unbound propagation of the exciton and the vibrational quanta in the crystal. Nevertheless, the authors of Refs. 2 and 3 noted relatively narrow absorption vibronic line corresponding to one-particle (bound) exciton-phonon states near the sum of FE's frequency and one vibrational quantum ($\omega \approx E_F/\hbar + \omega_0$). Our study confirms that conclusion about one-particle exciton-phonon state near vibronic with one phonon; however, the linear absorption near the frequencies of two- and three-phonon vibronics ($\omega \approx E_F/\hbar + m\omega_0, m=2, 3$) would exhibit wider absorption lines which correspond to MP exciton-phonon states.

Figure 1 concerns pure excitonic absorption. We calculate the excitonic and one-phonon vibronic spectra following Davydov-Serikov (DS) model¹⁰ and formula (A1). Then, we find the value of E'_F in Eq. (32) by fitting the calculated position of the excitonic level to coincide with the supposed excitonic level $E_F^{(0)} + 2L$ in Eq. (A1). Maxima 3 and 4 are obtained by using formulas (37) and (41), respectively, which accordingly are valid for two-phonon and three-phonon vibronic regions.

Figure 2 illustrates linear absorption in the one-phonon

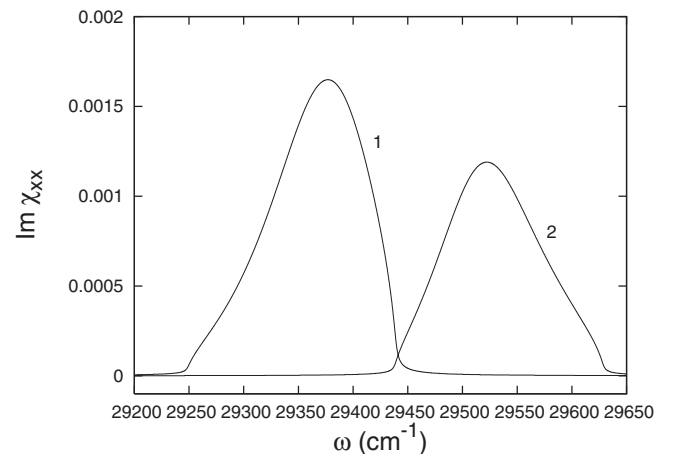


FIG. 5. Three-phonon vibronic region of anthracene for the same parameters as in Fig. 4.

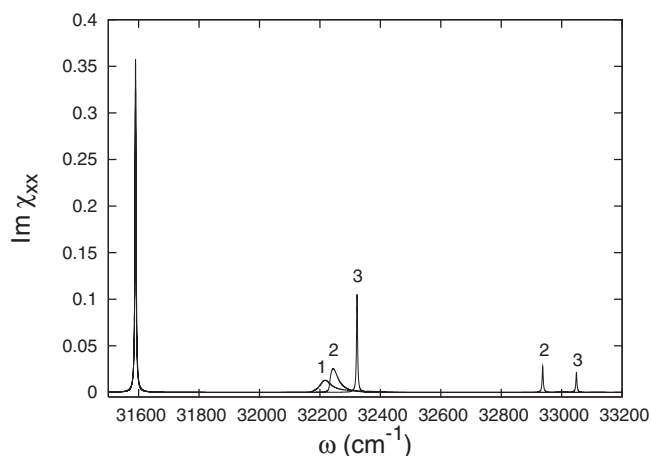


FIG. 6. Linear absorption spectra for one-dimensional model of naphthalene's crystal. Curve 1 is calculated by using Eq. (A1) with $L=45 \text{ cm}^{-1}$, curves 2 are calculated by using Eqs. (32) and (37), respectively, with $L=45 \text{ cm}^{-1}$, and curves 3 correspond to $L=-45 \text{ cm}^{-1}$. For the other parameters, see Table I. The three-phonon spectra are very weak and that is why they are not plotted in the figure.

vibronic region calculated by the DS model (curve 1 at $L > 0$ and curve 4 at $L < 0$) and on using our vibronic approach (curve 2 at $L > 0$ and curve 3 at $L < 0$). The DS model predicts wide many-particle bands [approximately with mirror symmetry with respect to the frequency $\omega = 26\,634 \text{ cm}^{-1} = (E_F^{(0)} + L)/\hbar + \omega_0$]. Our model leads to a different result, namely, the narrow absorption maximum at $L > 0$ proves to be a Lorentzian one and it corresponds to one-particle (bound) exciton-phonon state. The authors of Refs. 2 and 3 interpret the linear absorption one-phonon maximum as a quasibound exciton-phonon state inside the MP band. The relatively big linear exciton-phonon coupling ($\xi^2=0.9$) ensures a good metastability of the quasibound state near the sum of the frequencies of the Frenkel exciton and of the one

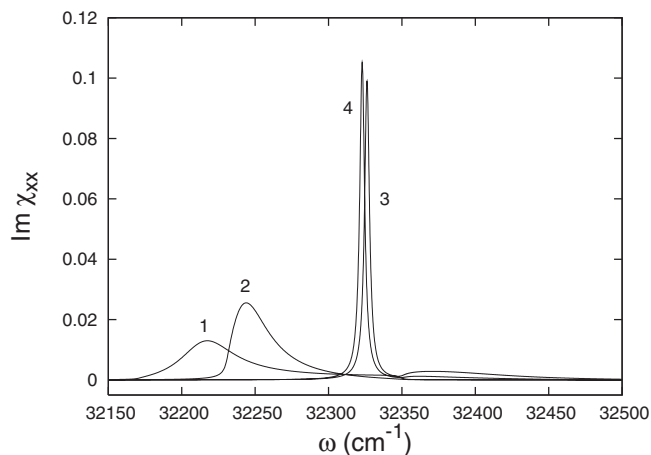


FIG. 7. One-phonon vibronic region of the linear absorption of naphthalene. Curve 1 corresponds to the DS model ($L > 0$), curve 2 is calculated using formula (32) at $L > 0$, curve 3 is according to the DS model with $L < 0$, and curve 4 is produced by formula (32) at $L < 0$.

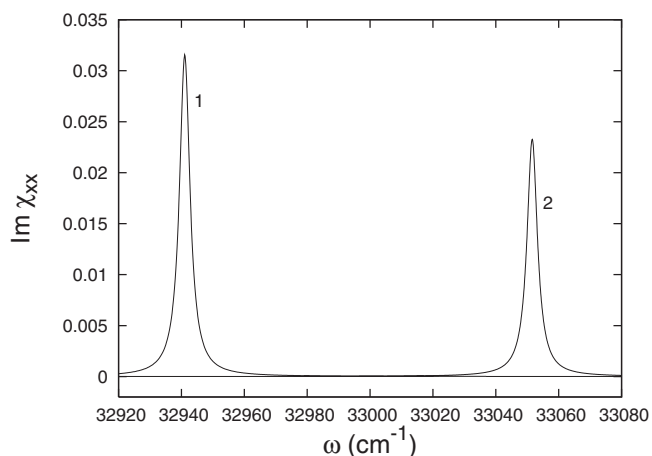


FIG. 8. Two-phonon vibronic region of naphthalene [see formula (37)]. Curve 1 corresponds to $L > 0$, while curve 2 to $L < 0$.

totally symmetrical vibrational quantum. The one-particle feature of the vibronic absorption is better expressed at $L > 0$ than at $L < 0$. In the last case, the width of the quasibound level is two times bigger than in the case of $L > 0$ (compare curves 2 and 3 in Fig. 2).

In Fig. 3, we compare the evolution of the absorption spectra calculated by using the DS model of a reduced Hamiltonian (48) which preserves the numbers of excitons and phonons in the crystal (curves 1–3) as well as by using our approach and the full Hamiltonian (8) (curves 4–6). All spectra have been calculated for $L=117 \text{ cm}^{-1}$; however, the exciton-phonon coupling constant ξ^2 has been supposed slightly to increase ($\xi^2=0.9, 1$, and 1.1 , respectively). In our model, the positions and amplitudes of the absorption maxima vary smoothly with the increasing of ξ^2 without any dramatic changes. In the DS model, the wide MP band (at $\xi^2=0.9$) is narrowed to a Lorentzian maximum at $\xi^2=1$ (the MP band disappears). Curve 3 ($\xi^2=1.1$) exhibits again one-particle maximum and a weak band at $\omega \approx 26\,630 \text{ cm}^{-1}$.

We also calculate the linear absorption in the two-phonon vibronic region (Fig. 4) and in the three-phonon vibronic region (Fig. 5). The very small values of the calculated ab-

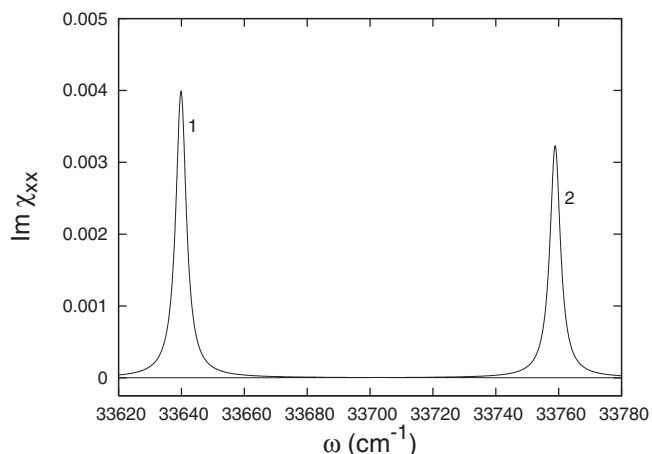


FIG. 9. Three-phonon vibronic region of naphthalene [see formula (41)]. Curve 1 corresponds to $L > 0$, while curve 2 to $L < 0$.

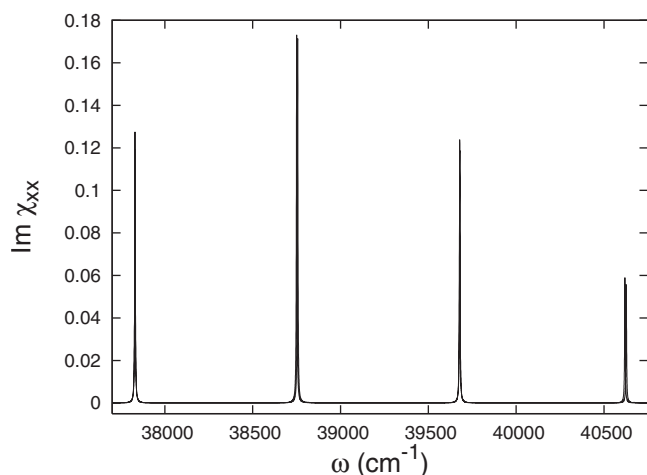


FIG. 10. Linear absorption spectra for one-dimensional model of benzene's crystal (see the parameters in Table I).

sorption in Fig. 5 explain the difficulties in the experimental observation of the three-phonon vibronic spectra. The absorption curves in both regions are asymmetrical ones and relatively wide. Their shape is more typical for MP bands deformed by the exciton-phonon coupling. In this way, our study yields a notable result: the intermediate ($\xi^2 \approx 1$) linear exciton-phonon coupling turns out to be enough for binding Frenkel exciton and one vibrational quantum, however, is not sufficient to bind the exciton and two (three) vibrational quanta.

B. Model of naphthalene absorption spectra

The model parameters for the crystal of naphthalene cited in Table I illustrate the case of relatively weak linear exciton-phonon coupling (in Ref. 3, the constant ξ^2 is evaluated even as equal to 0.2) and of comparable frequency shift $\hbar\Delta\omega$ and excitonic transfer integral L . It seems realistic to observe

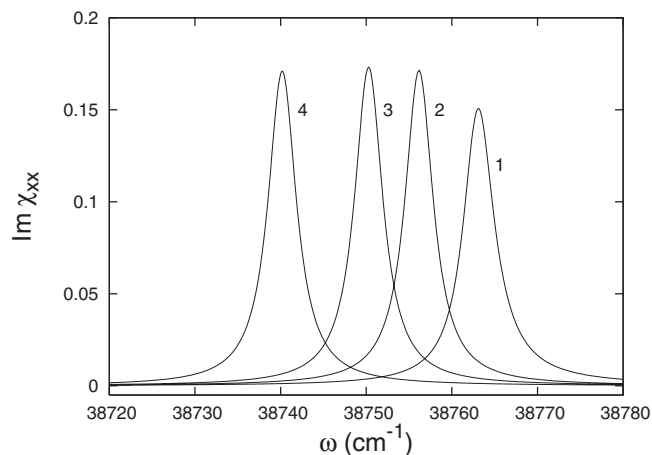


FIG. 11. One-phonon vibronic region of benzene's absorption spectra. Curve 1 is produced by the DS model ($L=15$ cm⁻¹), curve 2 is calculated from formula (32) at $L>0$, curve 3 is calculated from the same formula with $L<0$, and curve 4 is obtained from the DS model at $L<0$.

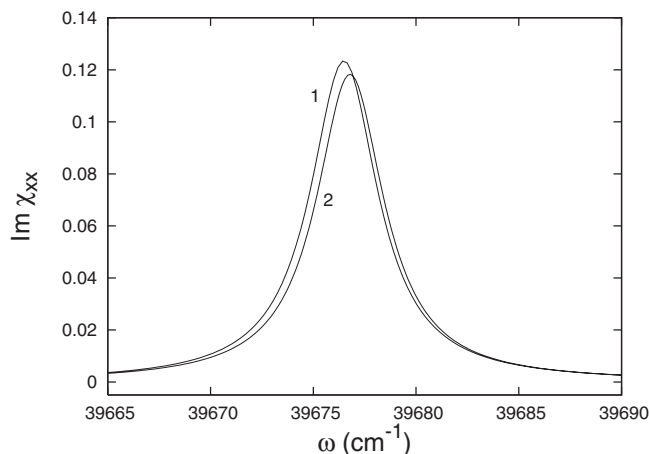


FIG. 12. Two-phonon (f_0) vibronic region of benzene [see formula (37)]. Curve 1 corresponds to $L>0$, while curve 2 to $L<0$.

linear absorption up to the two-phonon vibronic (Fig. 6).

One-phonon vibronic spectra turn out to be different depending on whether $L>0$ or $L<0$ (see Fig. 7). At $L>0$, both models—DS model and the vibronic one—yield an absorption line shape similar to the shape of the experimental absorption spectrum which consists of one broad MP band.^{2,3} Our calculations yield a band which is narrower and possesses a steeper left wing. There exists a surprising similarity between the absorption one-phonon vibronic spectrum calculated on the basis of our vibronic approach and the experimental data on the absorption in the same frequency region of 32 200–32 400 cm⁻¹ shown in Fig. 6.15 of Ref. 3. In the case of $L<0$, these MP bands are very weak and shifted beyond frequency $\omega \approx 32\,350$ cm⁻¹ but the two models predict intensive and practically coinciding one-particle absorption maxima below the MP band.

The two- and three-phonon vibronics both exhibit in the cases $L>0$ and $L<0$ narrow maxima which correspond to single-particle exciton-phonon states. Notably, such an absorption maximum appears near the frequency sum of FE + overtone of the totally symmetrical vibration of naphthalene's crystal at $\omega=32\,956$ cm⁻¹ (see Ref. 3). The distance

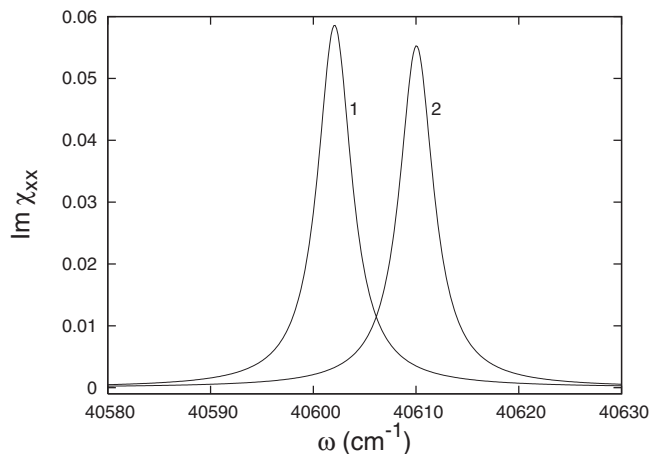


FIG. 13. Three-phonon vibronic region of benzene [see formula (41)]. Curve 1 corresponds to $L>0$, while curve 2 to $L<0$.

TABLE II. Parameters of the polymer models A, B, and C in Ref. 9. The values of L equal to -140 and -36.19 cm^{-1} correspond to -0.1 and -0.05 , respectively, in Ref. 9, while the values of the frequency ω_1 , 1400 and 723.81 cm^{-1} , correspond to 1 in the same reference.

Model	Free exciton level E'_F (cm^{-1})	Excitonic transfer integral L (cm^{-1})	Vibr. freq. in nonexcited molecule ω_0 (cm^{-1})	Constant of linear coupling ξ^2	Shift of the vibr. freq. in exc. molecule $\Delta\omega$ (cm^{-1})	Vibr. freq. in excited molecule ω_1 (cm^{-1})
A	26 700	-140	1400	0.3/0.7	0	1400
B	26 700	-140	1400	0.7/0.3	0	1400
C	31 800	-39.19	760	0.3/0.7	-36.19	723.81

between two-phonon and three-phonon maxima is approximately $\omega_1 \approx 700$ cm^{-1} . The binding of the exciton and two or more phonons is caused by the stronger impact of the quadratic coupling in the many-phonon vibronic spectra of naphthalene's crystal because the frequency shifts $2\hbar\Delta\omega$ [formula (40)] (Fig. 8) and $3\hbar\Delta\omega$ [formula (45)] (Fig. 9) strongly exceed the exciton transfer integral L .

C. Model of benzene absorption spectra

The model parameters of FE and totally symmetrical vibration of benzene (Table I) illustrate the occurrence of a narrow exciton band ($L=15$ cm^{-1}) and strong linear and quadratic exciton-phonon couplings. Thus, the absorption spectrum must be similar to the vibronic progression, namely, several intensive vibronic maxima separated by the distance $\hbar\omega_1 \approx \hbar(\omega_0 + \Delta\omega) \approx 923$ cm^{-1} (Fig. 10). The absorption curves in one-phonon vibronic spectra calculated by using the DS model (Fig. 11, curves 1 and 4) and from our model (curves 2 and 3) have close positions and amplitudes. We note the bigger energetic distance (approximately 25 cm^{-1}) between the two maxima predicted by the DS model in the

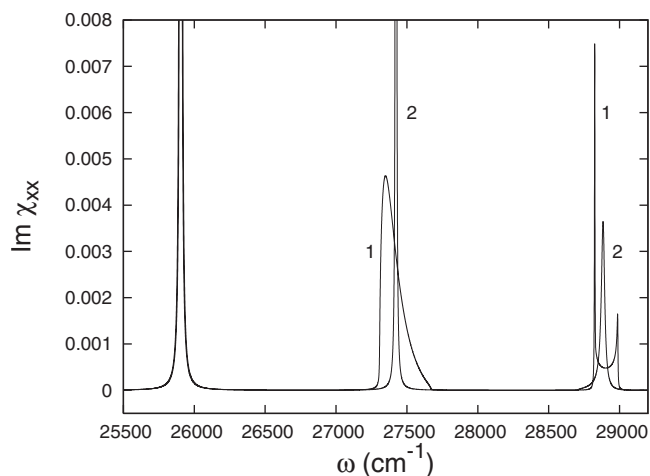


FIG. 14. Absorption spectra for polymer model A of Ref. 9 near the excitonic level (f_0) ($\approx 26\,000$ cm^{-1}), one-phonon vibronic level (f_1) ($\approx 27\,500$ cm^{-1}), and two-phonon vibronic level (f_2) ($\approx 29\,000$ cm^{-1}). Curve 1 has been calculated by using Eq. (32), while curve 2 has been obtained from Eq. (37).

cases of $L > 0$ and $L < 0$, respectively. The vibronic approach of the present paper in the case of a narrow benzene's exciton band is not sensitive to the sign of the quantity L not only in one-phonon vibronic spectra but also in two- (Fig. 12) and three-phonon (Fig. 13) vibronic spectra. The excitonic and vibronic spectra of the one-dimensional model of the benzene crystal exhibit maxima of the single-particle exciton-phonon states, in agreement with the available experimental data.^{2,3}

VI. COMPARISON WITH THE VIBRONIC SPECTRA CALCULATED IN REFERENCE 9

The calculations of the vibronic spectra in Ref. 9, based on a formalism different from our vibronic approach, concern the frequency regions of the Frenkel exciton and one- and two-phonon vibronics. Here, we calculate the vibronic spectra using formulas (32)–(45) in which we put the parameters for the three polymer models A, B, and C (i.e., one-dimensional ones) from Ref. 9 but for the case of inequality (30) that is basic in our study.

The constant ξ of the linear exciton-phonon coupling can be expressed through Franck-Condon overlap integrals,

$$\xi_{00,fm} = \int \chi^{(f,m)}(R) \chi^{(0,0)}(R) dR, \quad m = 0, 1, \dots, \quad (49)$$

where R is the vibrational normal coordinate, (0,0) is the ground electronic and vibrational state of the molecule, whereas (f,m) is the excited electronic state with m vibra-

TABLE III. Calculated integral intensities of the vibronic lines for polymer model A.

Line	Integral intensity according to Eq. (32) (curve 1 in Fig. 14) (arbitrary units)	Integral intensity according to Eq. (37) (curve 2 in Fig. 14) (arbitrary units)
Excitonic (zero-phonon)	2.241	2.268
One-phonon	0.704	0.683
Two-phonon	0.149	0.152
Three-phonon	0.023	0.025

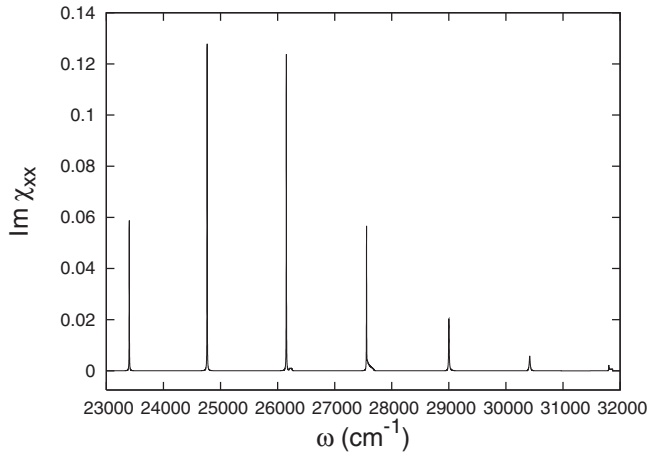


FIG. 15. Absorption spectra for polymer model B of Ref. 9 near the excitonic level ($\approx 23\,300\text{ cm}^{-1}$) and its five vibronic replicas calculated by using formula (37).

tional quanta. The functions χ denote the vibrational part of the corresponding wave functions in the Born-Oppenheimer approximation. The well-known expression for ξ^2 (see, for example, Refs. 2 and 8) has the form

$$\xi^2 = |\xi_{00,f1}/\xi_{00,f0}|^2. \quad (50)$$

Table II contains the parameters of the polymer models A, B, and C from Ref. 9 calculated in cm^{-1} for hypothetical one-dimensional crystals similar to those of anthracene and naphthalene (see Table I). Because of the big value of the constant ξ^2 for model B, we enlarge the ladders of calculations in formulas (32)–(45) up to 20 steps.

Figure 14 illustrates absorption in the case of model A. Curve 1, calculated by using Eq. (32), is more adequate to the one-phonon spectrum. The excitonic level ($f0$) corresponds to one-particle state, while the one-phonon spectrum ($f1$) represents a wide two-particle band (with width $\approx 400\text{ cm}^{-1}$) as it is in Ref. 9. The same formula (32) yields as a two-phonon vibronic spectrum another continuum with a “spike” absorption near its ends (compare with Fig. 5 of Ref. 9, calculated for the same values of the parameters but for a three-dimensional model). We emphasize that the adequate absorption curve for the two-phonon vibronic region is curve 2 in Fig. 14 calculated from formula (37). It exhibits

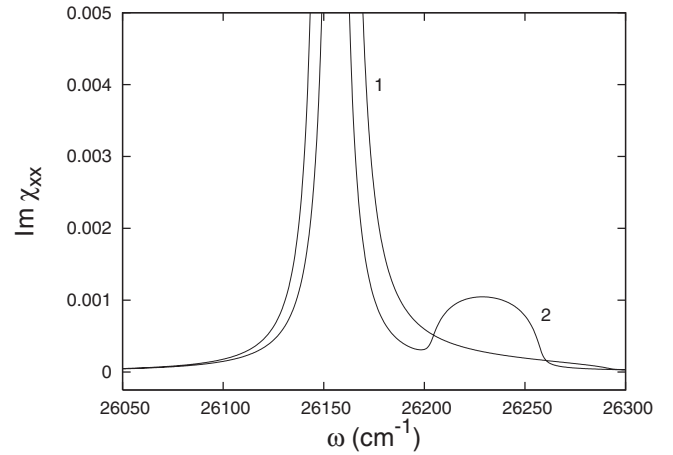


FIG. 16. Absorption spectra for polymer model B of Ref. 9 near the two-phonon vibronic level. Curve 1 is derived from formula (32) and curve 2 is calculated by using formula (37) describing the two-phonon vibronic spectrum.

nearly single-particle absorption spectrum near the sum of the frequencies of the exciton plus two phonons. The creation of the single-particle state which consists of one exciton plus two vibrational quanta is mainly due to the opportunity to excite a twofold vibrational excitation on the molecule with an electronic excitation. The approach of Ref. 9 treats a case in which the two vibrational quanta are excited on different molecules [see Eq. (2.16) in Ref. 9] and thus a multiparticle manifold like curve 1 is more probable than curve 2.

Despite the different formulas and as a consequence the different shapes of the vibronic lines, the integral intensities of the zero-, one-, two-, and three-vibronic lines derived from formulas (32) and (37) differ by several percents only (see Table III).

The large magnitude of $\xi^2=2.333(3)$, the constant of the linear exciton-phonon coupling for model B, causes the appearance of several vibronic lines with $m=1,2,\dots,5$ vibrational quanta (see Fig. 15). The strong exciton-phonon coupling is also the reason for the single-particle shape of the absorption lines. Practically, the two-particle continuum could be seen in the two-phonon region only (see Fig. 16) but its integral intensity represents 7% of the integral intensity of the single-particle state at $26\,150\text{ cm}^{-1}$. We note that

TABLE IV. Calculated integral intensities of the vibronic lines for polymer model B.

Line	Integral intensity according to Eq. (32) (arbitrary units)	Integral intensity according to Eq. (37) (arbitrary units)	Integral intensity according to Eq. (41) (arbitrary units)
Excitonic (Zero-phonon)	0.370	0.368	0.368
One-phonon	0.797	0.800	0.802
Two-phonon	0.820	0.765 single-particle line 0.052 two-particle band	0.816
Three-phonon	0.575	0.575	0.578
Four-phonon	0.322	0.324	0.324
Five-phonon	0.151	0.152	0.156

TABLE V. Spectral positions and integral intensities of the absorption maxima calculated by means of formula (32) for polymer model C.

Line	Position (cm ⁻¹)	Integral intensity (arbitrary units)
Excitonic (Zero-phonon)	31 441	2.135
One-phonon	32 186 single-particle line 32 200–32 300 two-particle band	0.123
Two-phonon	32 931	0.146
Three-phonon	33 660	0.023

the details on curve 2 (which describes notably two-phonon spectra) disappear on curve 1, the main view of which is that of one-phonon spectrum. On the other hand, the wing of the three-phonon maximum near 27 500 cm⁻¹ is missing in calculating the absorption using formula (41) that describes notably three-phonon vibronic spectra.

The significant integral intensities of the several vibronic lines have been calculated by using formulas (32), (37), and (41) (see Table IV). They confirm the self-consistency of the different formulas with some deviations from the ratios of the integral intensities calculating with the help of formula (47). These deviations are due to the intermediate values of the exciton transfer integral L .

Polymer model C illustrates the simultaneous impact of the linear and quadratic exciton-phonon couplings. The calculations show predominantly a single-particle shape of the absorption spectra (see Table V). The vibronic spectrum ($f1$) is the only region where a single-particle state as well as a two-particle band could be observed in the absorption (see Fig. 17). In such a way, our calculations confirm the results obtained by Philpott⁹ for the vibronic spectrum of model C (see Table 4 and Fig. 11 of Ref. 9). Moreover, the gap between the two single-particle states ($f0$) and ($f1$) according to Ref. 9 would be

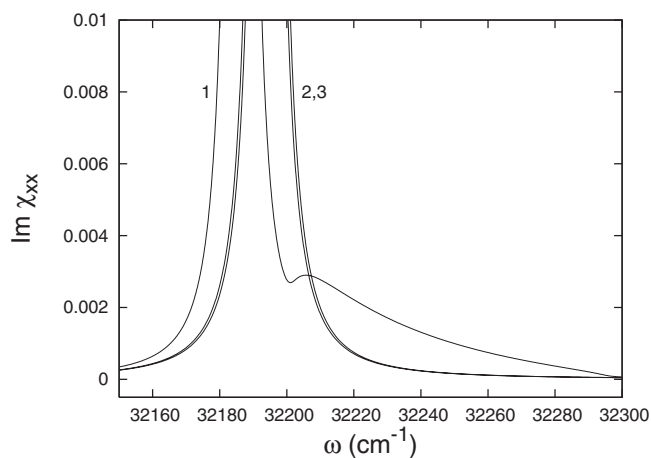


FIG. 17. Absorption spectra for polymer model C of Ref. 9 near the one-phonon vibronic line. Curve 1 is obtained from formula (32), while the coinciding curves 2 and 3 have been calculated by using formulas (37) and (41), respectively.

$$E(m=1) - E(m=0) = 0.954\,25 - (-0.073\,28) = 1.027\,53.$$

We choose for model C an energy span of 723.81 cm⁻¹, so the gap between these two states turns to be 743.37 cm⁻¹. We obtain for the same gap (see Table V) 745 cm⁻¹. Practically, the ratios of the integral intensities of the two single-particle states obtained from our calculations and those derived in Ref. 9 coincide, too (3.320 and 3.362, respectively).

We conclude this section by comparing the general pictures of the vibronic spectra obtained using our approach and that developed in Ref. 9. The two ways of calculations yield similar results concerning excitonic line ($f0$) and the first vibronic replica ($f1$) but the vibronic approach in our study seems to be more compact giving single-particle as well as multiparticle spectra. It is more easy to extend the applicability of our approach to more complicated vibronic complexes with two, three, and so on phonons by taking into account the excitation of one exciton and several phonons on one molecule. Any limitations on the values of exciton-phonon coupling constants do not appear; however, the inclusion of the important case of wide exciton bands [where inequality (30) is not valid] requires a further improvement of mathematics in both approaches.

VII. CONCLUSION

In this paper, we develop the vibronic approach of investigating the excitonic and vibronic spectra of molecular crystals. This approach avoids the separation of the problem into subproblems with different numbers of assisted phonons which is an approximate procedure. There exists only one real limitation for applicability of that approach: notably, the width of the excitonic bands must be smaller compared with the energy of the vibrational quanta (which is a specific feature of the so called *dynamical theory of the vibronic spectra*^{3,8,10}). In such a way, we make a complete and compact calculation of the absorption spectra in the excitonic and in different vibronic regions introducing the excitonic and vibronic parameters of some well-known aromatic crystals, anthracene, naphthalene, and benzene, as well as of the models of crystals considered in Ref. 9. Our model is one-dimensional but it can be applied for studying three-dimensional anisotropic crystals.

The several main results of our study are as follows.

(1) We modify the dynamical approach and find out analytical expressions for the linear optical susceptibility and the absorption coefficients in pure excitonic and one-phonon vibronic as well as two- and three-phonon vibronic spectra. These self-consistent expressions connect the many-phonon vibronic regions and the excitonic spectra. There are no principal obstacles to apply the same vibronic approach to dealing with four-phonon, five-phonon, and so on vibronic spectra (if necessary).

(2) The linear exciton-phonon coupling governs the integral intensity of excitonic, one-phonon, two-phonon, three-phonon, and so forth vibronic frequency regions conforming to the rule of vibronic progression (47). That intensity is distributed between the single-particle and many-particle exciton-phonon states. An intermediate linear exciton-

phonon coupling only can bind the exciton and one vibrational quantum but it is not sufficient to create the bound exciton-phonon states with two, three, etc., vibrational quanta (see the absorption spectra of anthracene). The stronger linear exciton-phonon coupling creates predominantly single-particle exciton-phonon states (model B in Sec. VI).

(3) The role of the quadratic exciton-phonon coupling, manifesting itself through the shift of the vibrational frequency in the excited molecule, increases in the two-phonon, three-phonon, and so on vibronic spectra. The model of naphthalene and the calculations in Sec. VI represent an example of relatively weak linear coupling and comparable values of the exciton mobility parameter and vibrational frequency shift. The one-phonon vibronic spectrum consists of one broad band of unbound exciton and phonon, whereas the stronger quadratic coupling creates Lorentzian maxima of the bound exciton-phonon states in the two-phonon, three-phonon, and so forth vibronic spectra.

(4) The value $\xi^2=1$ is considered as a boundary between the intermediate and strong linear exciton-phonon couplings. Our calculations do not demonstrate its special role in the analytical treatment of the one-phonon vibronic spectrum as it is in the one-dimensional DS model.¹⁰ We stress on the adequacy of the model of the intermolecular exchange of the whole vibronic excitations (7) and not of separate exciton-phonon complexes [compare the Hamiltonians (8) and (48)].

The version of the vibronic approach presented in this paper treats the vibronic excitations with the participation of one mode of the totally symmetrical molecule's vibration. We mention two directions of a further development of the present theory. (i) One is the linear absorption near vibronic spectra of composite tones,^{2,3,19} i.e., near the sum of frequencies of a Frenkel exciton plus two (or more) different vibra-

tional quanta (one of them can originate from non-totally-symmetric vibrations of the molecules). The observation of vibronics with composite tones in naphthalene's crystal (see Ref. 3, Sec. 6.4.4) can stimulate a corresponding theoretical investigation. (ii) The anharmonicity may be important in the vibronic spectra with two or more vibrational quanta.¹⁹ The inclusion of anharmonicity will represent an extension of the vibronic approach (if the magnitude of anharmonicity is comparable to the frequency shift in a molecule with FE).

APPENDIX

The linear optical susceptibility in Davydov-Serikov model¹⁰ has been calculated by using a method analogous to that in the present paper, but the Hamiltonian has been modified to preserve the numbers of excitons and phonons in the crystal and adapted for dealing with one-phonon vibronic spectrum only [see formula (48)]. Davydov and Serikov obtain the following expression for the linear optical susceptibility (we use the notation of the present paper):

$$\chi_{xx} = -\frac{P_F^2 N}{\hbar V} \exp(-\xi^2) \left\{ \frac{1}{\hbar\omega - E_F^{(0)} - 2L} + \xi^2 \frac{\sigma - \xi^2 \sigma_1}{2LD_s} \right\}, \quad (\text{A1})$$

where

$$D_s = 1 - [\xi^2 + \hbar\Delta\omega/(2L)]\sigma(t) - \xi^2\sigma_1(t)[-2 + t - \hbar\Delta\omega/(2L)],$$

$$t = (\hbar\omega - E_F^{(0)} - \hbar\omega_0)/(2L), \quad \sigma_1(t) = t\sigma(t) - 1,$$

$$\sigma(t) = \begin{cases} -1/\sqrt{t^2 - 1} & \text{if } |t + \sqrt{t^2 - 1}| < 1 \\ 1/\sqrt{t^2 - 1} & \text{if } |t + \sqrt{t^2 - 1}| > 1. \end{cases}$$

¹A. S. Davydov, *Theory of Molecular Excitons* (Plenum, New York, 1971).

²E. F. Sheka, *Sov. Phys. Usp.* **14**, 484 (1972).

³V. L. Broude, E. I. Rashba, and E. F. Sheka, *Spectroscopy of Molecular Excitons* (Springer, Berlin, 1985).

⁴G. Herzberg, *Molecular Spectra and Molecular Structure. II. Infrared and Raman Spectra of Polyatomic Molecules* (Van Nostrand, New York, 1945).

⁵H. Sponner, G. Nordheim, A. L. Sklar, and B. Geller, *J. Chem. Phys.* **7**, 207 (1939).

⁶D. E. Freeman, *J. Mol. Spectrosc.* **6**, 305 (1961).

⁷O. P. Kharitonova, *Opt. Spectrosc.* **5**, 29 (1958).

⁸E. I. Rashba, *Sov. Phys. JETP* **23**, 708 (1966); **27**, 292 (1968).

⁹M. R. Philpott, *J. Chem. Phys.* **55**, 2039 (1971).

¹⁰A. S. Davydov and A. A. Serikov, *Phys. Status Solidi* **42**, 603 (1970); *Phys. Status Solidi B* **44**, 427 (1971).

¹¹I. J. Lalov, K. T. Stoychev, and S. P. Penchev, *Phys. Status Solidi B* **120**, 671 (1983).

¹²M. Hoffmann, Z. G. Soos, and K. Leo, *Nonlinear Opt.* **29**, 227 (2002), doi:10.1080/1058726021000044514.

¹³I. J. Lalov and A. I. Miteva, *J. Chem. Phys.* **87**, 6334 (1987).

¹⁴M. Hoffmann and Z. G. Soos, *Phys. Rev. B* **66**, 024305 (2002).

¹⁵I. J. Lalov and I. Zhelyazkov, *Phys. Rev. B* **74**, 035403 (2006).

¹⁶V. M. Agranovich, in *Spectroscopy and Exciton Dynamics of Condensed Molecular Systems*, edited by V. M. Agranovich and R. M. Hochstrasser (North-Holland, Amsterdam, 1983), p. 83.

¹⁷I. J. Lalov and I. Zhelyazkov, *Chemical Phys. Research J.* (to be published).

¹⁸A. S. Davydov, *Solid State Theory* (Nauka, Moscow, 1976) (in Russian).

¹⁹I. J. Lalov, *Phys. Status Solidi B* **68**, 319 (1975); **68**, 681 (1975).